Since January 2020 Elsevier has created a COVID-19 resource centre with free information in English and Mandarin on the novel coronavirus COVID-19. The COVID-19 resource centre is hosted on Elsevier Connect, the company's public news and information website.

Biochimica et Biophysica Acta 1858 (2016) 30–37

Contents lists available at ScienceDirect

Biochimica et Biophysica Acta

journal homepage: www.elsevier.com/locate/bbamem

Ion channel activity of the CSFV p7 viroporin in surrogates of the ER lipid bilayer

Eneko Largo [a], Carmina Verdiá-Báguena [b], Vicente M. Aguilella [b], José L. Nieva [a], Antonio Alcaraz [b,*]

[a] Biophysics Unit (CSIC, UPV/EHU), Department of Biochemistry and Molecular Biology, University of the Basque Country (UPV/EHU), P.O. Box 644, 48080 Bilbao, Spain
[b] Laboratory of Molecular Biophysics, Department of Physics, University Jaume I, 12071 Castellón, Spain

ARTICLE INFO

Article history:
Received 8 July 2015
Received in revised form 8 October 2015
Accepted 9 October 2015
Available online 14 October 2015

Keywords:
Viroporins
Ion channels
Planar membranes
Lipid vesicles

ABSTRACT

Viroporins comprise a family of non-structural proteins that play significant and diverse roles during the replication cycle of many animal viruses. Consequently, they have become promising targets for inhibitory drug and vaccine development. Structure–function traits common to all members of the family are their small size (ca. 60–120 aa), high hydrophobicity, and the presence of helical domains that transverse the membrane and assemble into oligomeric-permeating structures therein. The possibility that viroporins show in particular conditions any kind of specificity in the transport of ions and small solutes remains a point of contention in the field. Here we have approached this issue using the Classical Swine Fever Virus (CSFV) protein p7 viroporin as a model. We have previously reported that CSFV-p7 induces release of ANTS (MW: 427.33) from lipid vesicles that emulate the Endoplasmic Reticulum (ER) membrane, and that this process is dependent on pH, modulated by the lipid composition, and recreated by a C-terminal transmembrane helix. Here we have assayed CSFV-p7 for its capacity to form ion-conducting channels in ER-like planar lipid membranes, and established whether this activity is subject to regulation by the same factors. The analysis of electrophysiological recordings in ER membrane surrogates suggests that CSFV-p7 forms pores wide enough to allow ANTS release. Moreover, we were able to discriminate between two pore structures with slightly different sizes and opposite ion selectivities. The fact that the relative abundances of each pore type depend crucially on membrane composition strengthens the view that the physicochemical properties of the lipid bilayers present in the cell endomembrane system modulate viroporin activity.

1. Introduction

Modulation of the cellular ion balance in order to take over the cellular machinery seems to be a common feature for viruses. Several viruses encode at least one protein displaying ion channel (IC) activity. These proteins are known as viroporins, the term being first proposed when it was observed that several proteins involved in virus-promoted cell membrane permeabilization shared common characteristics [1]. The list of identified viroporins is constantly growing, especially in RNA viruses [2,3]. Thus, the M2 of influenza virus (IFV) [4–7], the p7 of hepatitis C virus (HCV) [8–12], the vpu of human immunodeficiency virus (HIV) [13–17], and the poliovirus (PV) 2B [18–21] proteins are only some members of this list found in prominent human pathogens. Accordingly, viroporin activity blocking by specific inhibitors, and viroporin-defective live attenuated vaccines offer new therapy approaches to treat and prevent viral infection, which reinforces the importance of investigating these proteins [2].

Viroporins are overall small (they are comprised of some 60–120 amino acids) and highly hydrophobic. They usually contain one (class I) or two (class II) α-helices long enough to transverse the lipid bilayer [2,22]. These features enable viroporin insertion and oligomerization in cell membranes forming ion conductive pores, which alters the cell permeability allowing the transport of ions and other small molecules. The IC activity of these proteins is expected to be involved in virus entry, trafficking, morphogenesis and maturation [23,24]. In fact, research work supports the relevance of the IC activities of IFV M2 [25–28], HCV p7 [29–31], or SARS-CoV E [32] proteins in virulence and pathogenesis.

IC activity of viroporins usually involves weakly selective nanopores that alter unspecifically the membrane permeability, i.e. they allow the transport of ions and small molecules irrespective of their chemical nature [32]. However, in some particular cases like IFV M2 and HCV p7, they can form highly selective channels displaying specificity for physiologically relevant cations [4–7,33,34]. Given the varied functions ascribed to viroporins and the various cell environments sampled by these products, it is not unlikely that different functional structures can emerge at different stages of the viral cycle. One consequence of this functional diversity is the possibility that depending on the conditions

* Corresponding author.
E-mail address: alcaraza@uji.es (A. Alcaraz).

http://dx.doi.org/10.1016/j.bbamem.2015.10.007
0005-2736/

of the lipid bilayer the same viroporin may have the potential either to establish nanometer-sized ion channels, or alternatively, participate in additional membrane permeabilization mechanisms allowing the transport of larger solutes exceeding the nanometer scale [35,36].

Interestingly, it has been observed that lipid charge influences the IC activity of some viroporins like the E protein of SARS-CoV [32], while vesicle permeabilization assays suggest that PV 2B pore-forming activity can be regulated by the negatively charged phospholipid species existing at the cytofacial monolayers of the target membranes [37]. However, studies addressing in parallel and systematically (i.e., using same lipid compositions and assessing dependence of these activities on the same regulatory factors) planar membrane electrophysiology vs. vesicle permeability assays for the same viroporin are missing. Here, to carry out such a comparative assessment, we have taken the advantage that CSFV-p7-induced release of ANTS from lipid vesicles mimicking the Endoplasmic Reticulum (ER) membrane is subject to pH, lipid composition and amino acid sequence regulation [38]. Thus, we have first established IC activity of CSFV-p7 in ER-like lipid planar bilayers and then analyzed its dependence on the same factors.

2. Materials and methods

2.1. Materials

The CSFV p7 protein and its derived peptides (sequences displayed in Fig. 1) were commercially synthesized (Thermo Scientific). The purified peptides were dissolved in dimethyl sulfoxide (DMSO; spectroscopy grade), and their concentrations were determined by bicinchoninic acid microassay (Pierce, Rockford, IL). Small, diluted aliquots were stored frozen upon use. Phosphatidylcholine (PC), phosphatidylethanolamine (PE), phosphatidylinositol (PI), and cholesterol (Chol) were purchased from Avanti-Polar Lipids (Birmingham, AL). The 8-aminonaphthalene-1,3,6-trisulfonic acid sodium salt (ANTS) and p-xylenebis(pyridinium)bromide (DPX) were obtained from Molecular Probes (Junction City, OR, USA).

2.2. Planar lipid membranes formation

Two monolayers were made from 5 mg/ml pentane solutions of lipid mixture buffered with 5 mM HEPES with KCl at both sides of Teflon chambers partitioned by a 15 μm thick Teflon film with 70–100 μm diameter orifices. Planar lipid bilayers were formed by monolayer apposition on the orifices previously treated with a 1% solution of hexadecane in pentane. Protein and peptides dissolved in DMSO were supplemented to the lipid solutions prior to monolayer formation only in one of the chamber sides, the *cis* side. Bilayer formation was directly detected and its thickness can be estimated by capacitance measurements.

2.3. Channel conductance measurements

An electric potential was applied using Ag/AgCl electrodes in 2 M KCl, 1.5% agarose bridges assembled within standard 250 μl pipette tips. Potential is defined as positive when it is higher at the side of the protein addition (the *cis* side), while the *trans* side is set to ground. An Axopatch 200B amplifier (Molecular Devices, Sunnyvale, CA) in the voltage-clamp mode was used for measuring the current and applying potential. The membrane chamber and the head stage were isolated from external noise sources with a double metal screen (Amuneal Manufacturing Corp., Philadelphia, PA).

2.4. Reversal potential measurements

Lipid bilayers were formed with different salt concentrations at each side. Once the protein was inserted, a net ionic current appeared due to the concentration gradient, and it was manually set to zero by adjusting the applied potential. The potential needed to achieve zero current was then corrected by the liquid junction potential calculated from Henderson's equation to obtain the zero current potential or reversal potential (E_{rev}) [39].

2.5. Vesicle permeability assays

Large unilamellar vesicles (LUVs) were prepared according to the extrusion method [40]. Vesicle permeabilization was assayed by monitoring the release to the medium of encapsulated fluorescent ANTS (ANTS–DPX assay) [41]. LUVs containing 12.5 mM ANTS, 45 mM DPX, 20 mM NaCl and 5 mM HEPES were obtained by separating the unencapsulated material by gel-filtration in a Sephadex G-75 column that was eluted with 5 mM HEPES and 100 mM NaCl (pH 7.4). Internal and external osmolarities were measured in a cryoscopic osmometer (Osmomat 030, Gonotec, Berlin, Germany) and adjusted by adding NaCl. Fluorescence measurements were performed in an SLM Aminco 8100 spectrofluorimeter (Spectronic Instruments, Rochester, NY) by setting the ANTS emission at 520 nm and the excitation at 355 nm. A cutoff filter (470 nm) was placed between the sample and the emission monochromator. The baseline leakage (0%) corresponded to the fluorescence of the vesicles at time 0, while 100% leakage was the fluorescence value obtained after the addition of Triton X-100 (0.5% v/v).

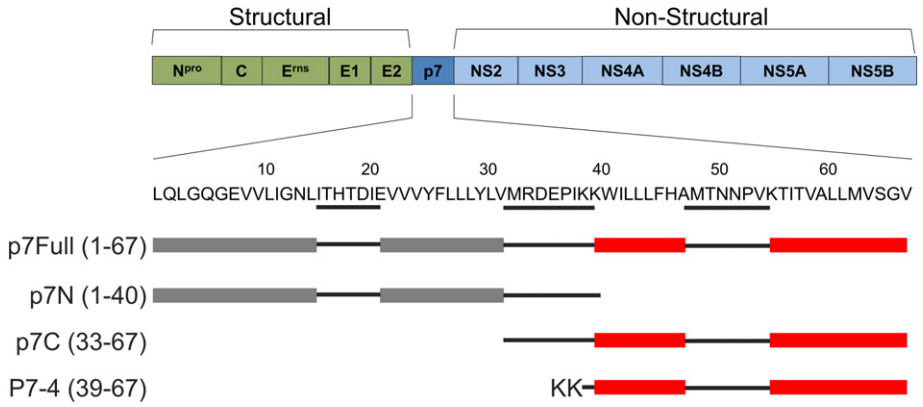

Fig. 1. CSFV p7 sequence and derived peptides. Top: Direct translation of pestivirus ssRNA genome gives rise to a single, large polyprotein, which is processed into individual viral proteins (Top panel). Bottom: CSFV p7 sequence includes two main hydrophobic regions (gray and red blocks, respectively) intervened by sections with propensity for establishing turns in membrane (black, thick lines). The panel displays in schematic representation the sequences covered by the peptides used in this study.

2.6. Statistical processing

For comparison between vesicle leakage and channel formation activity, two kinds of assays were performed. For vesicle leakage results, at least four kinetic assays were performed and shown data correspond to arithmetic mean and standard error. In case of channel formation activity, 30 recordings comprising 10 traces with a duration of 20 s were analyzed. Each trace with at least one 2 pA event was considered as positive. The histograms of the current jump amplitude were made from at least 60 recordings and more than 550 events were analyzed for each histogram. The data were normalized to 1, using the number of total events in each case. The histograms were fitted to one or two Gaussian peaks, depending on the value of the adjusted R-squared. Each SD value is the square root variance of the corresponding Gaussian distribution. The histograms of permeability ratio contain data from 64 recordings.

3. Results and discussion

3.1. Ion channel activity of CSFV-p7

The CSFV-p7 protein possesses two hydrophobic, membrane-spanning regions (TM1 and TM2) separated by a short basic loop, an arrangement characteristic of class II viroporins (Fig. 1). Each hydrophobic domain is additionally intervened by a short loop with polar character, a feature also shared by integral membrane proteins that assemble into helical oligomers [22]. CSFV-p7 induces ANTS release from liposomes, a process that requires acid pH and evolves more efficiently in ER-like membranes [38,42]. The pore-forming activity and its regulation by pH and lipid composition can be recreated by the p7C peptide, representing the C-terminal domain including the TM1–TM2 connecting basic loop (Fig. 1). In order to improve the topological localization of the viroporin activity, p7-4, a TM2-based peptide lacking the basic loop, was designed. Interestingly, p7-4 also induces ANTS release from liposomes, but the process does not require acid pH and it is not inhibited by classic viroporin inhibitors [42]. These previous results could indicate that the TM1–TM2 connecting loop is essential for the CSFV-p7 activity regulation. Up to date, CSFV-p7 full protein and its constituent domains have been shown to participate in the permeabilization of lipid vesicles [38], but electrophysiological measurements investigating their pore-formation mechanisms at the single channel level are missing.

To this end, CSFV p7 viroporin was first assayed in planar lipid mixtures that mimicked the composition of ER membranes (Fig. 2). Although the ER is the main site of cholesterol and structural phospholipid synthesis, these lipids are rapidly transported to other organelles and, in fact, ER displays only low concentrations of sterols and complex sphingolipids [43]. Accordingly, we prepared planar bilayers based on the main constituent phospholipids of the ER membrane, namely, zwitterionic PC and PE plus the anionic PI mixed in a roughly 5:3:2 molar ratio [43].

In experiments performed in 150 mM KCl and pH 5.0 the complete protein (p7Full) exhibited a high IC activity with a variety of current levels and lifetimes (Fig. 2). In those experiments different kinds of events appear. On the one hand, traces showing well-defined "opening" and "closing" rapid events, and on the other hand, larger current levels with longer lifetimes without almost any small flickering (Fig. 2A). This effect could be due to the simultaneous opening of several channels or could correspond to the formation of different channel structures. In order to discriminate between single and multiple channel insertions, the analysis of all recordings allowed resolving the stepwise changes (ΔI) in each trace. The current vs. time traces were analyzed with the software Clampfit 10.1, so that average current values for each level were obtained once the corresponding zero-voltage baseline was subtracted. Histograms of the current jump amplitudes of the recorded

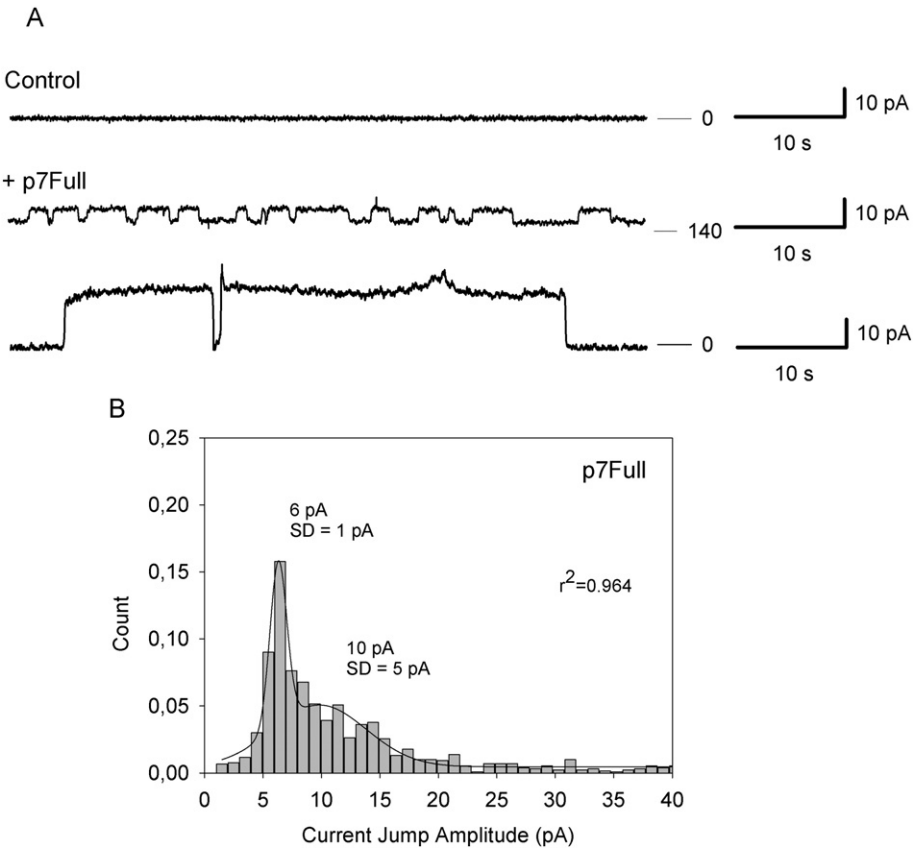

Fig. 2. CSFVp7 ion channel activity in ER-like planar bilayers. A) Current recordings without any protein addition (Control) and after the addition of p7Full protein. Two representative traces of the p7Full ion channel activity are chosen to show the different magnitudes of current jumps seen in experiments. B) Histogram of the current jump amplitude fitted to two Gaussian peaks (6 pA, SD = 1 and 10 pA, SD = 5). Current was recorded in 150 mM KCl, pH 5.0 at a potential of −50 mV.

traces (Fig. 2B) showed the most frequent events corresponding to a single channel current of 6 ± 1 pA, although the presence of a dim shoulder around 10 pA suggested some contribution from concatenated channels (see below).

Since current traces were recorded under an applied voltage of 50 mV our results point to a single channel conductance $G = 120 \pm 20$ pS, similar in value to that of SARS-CoV E viroporin [32]. Assuming as a first approximation cylindrical geometry for the permeating structure, the conductance can be written as $G \sim \kappa\pi r^2 / L$ where κ is the electrolyte conductivity and L the pore length. This allows for a rough estimation of the channel radius of $r \sim 0.5$–1 nm. In the context of protein channels, this is a relatively wide pore comparable in size to general diffusion porins [44]. In principle, CSFV-p7 channels formed under these conditions should permit simultaneous transport of water molecules, solvated ions and even small solutes such as ANTS [45].

Next we studied the effect of pH on the membrane permeabilization induced by CSFV p7 viroporin, paying attention to both current recordings in planar membranes and leakage experiments in LUVs. For the sake of comparison, in Fig. 3 we plot together the relative number of channel insertions (regardless of the actual current value) and the ANTS leakage measured in LUVs. We observe a sound qualitative correlation between both techniques (left panels). At pH 5.0 in ER membranes the high pore-forming activity observed in planar membranes is consistent with a large leakage value. Furthermore, when the pH is increased to 7.4, the remarkable decrease in recordings displaying ion channel activity is in agreement with the almost inexistent leakage found in LUVs. Of note, single channel currents of 6 pA or larger were occasionally found in the recordings at neutral pH (less than 25% of the total events, see right panels).

Interestingly, the pH is not the only critical parameter controlling ion channel activity but the membrane composition is also crucial. Previous work demonstrated that the lack of anionic phospholipids in the lipid composition, abated p7 permeabilizing activity measured in vesicles [38,42]. Control experiments performed in a 3-lipid PC:PE:Chol (7:3:10 molar ratio) mixture at pH 5.0 showed only tiny currents, which is also compatible with the small leakage found in LUVs of similar composition. By selecting this control mixture, it was not our intention to analyze the effects of cholesterol on channel activity (this would require thorough analysis, which was beyond the scope of the present work), but rather to test the absence of the anionic phospholipid PI. In fact, similar results were obtained in the absence of cholesterol using PC:PE (7:3 molar ratio) planar bilayers (data not shown).

3.2. Sequences involved in CSFV-p7 ion channel activity

The CSFV p7 IC activity observed in the previous experiments might depend on sequences different to those sustaining vesicle permeabilization [38,42]. Thus, to map IC activity, CSFV p7 sequence-based peptides were synthesized and analyzed in planar bilayers resembling ER composition. As displayed in the diagram of Fig. 1, p7N and p7C sequences spanned the potential N- and C-terminal TM1 and TM2 regions of CSFV p7, respectively, and overlapped along the conserved polar loop sequence [38]. In the case of p7-4, the sequence was selected to span the hydrophobic C-terminal TM2 of CSFV p7. The resulting sequence was long enough to transverse the membrane, although interrupted by the turn-promoting ^{49}MTNNPVK^{55} polar sequence. The pore-forming activities of these peptides were assessed in artificial lipid bilayers, as shown in Fig. 4A. Both p7C and p7-4 peptides exhibited substantial IC activity, in agreement with the high values of leakage induced by these peptides in LUVs. In contrast, p7N showed almost null currents both in electrophysiological recordings and in LUVs. These data confirm a similar dependence of vesicle permeabilization and IC activities on the C-terminal helix of CSFV-p7.

However, the histograms of the current jump amplitudes of the recorded traces denoted certain differences between the IC activities displayed by p7C and p7-4 (Fig. 4B). Whereas p7C recreated with remarkable accuracy p7full behavior (i.e., a prevalent single channel current of ca. 6 pA and a shoulder at 10–12 pA), p7-4 favored lower intensity currents of ca. 2–3 pA and no evidence for a bias towards a larger structure could be found in the histogram. Thus, the addition of the ^{33}MRDEPI^{38} turn sequence seems to be required for precisely recapitulating p7full IC activity by the TM2-based peptides. This observation was further supported by the next set of experiments.

Next we tested the dependence of p7C and p7-4 IC activities on solution pH and membrane composition, as previously done in the case of the full protein (Fig. 3). Interestingly, each peptide's IC activity seems to display a particular behavior, which was mirrored by their effects on vesicle leakage. On the one side, p7C performs like the full CSFV p7 protein both in LUVs and in electrophysiological recordings (Fig. 5A). On the other side p7-4 shows a distinctive feature in ER membranes. Increasing pH does not inhibit the ability of p7-4 to induce membrane permeabilization (Fig. 5B). This seems a particular characteristic of ER membranes, because PI lacking control membranes show in both peptide samples very low currents at pH 5. The ANTS leakage induced by p7-4 also shows a significant reduction under these conditions as compared to PI-containing samples. Although the reduction in leakage is not so marked, once again, the correlation between planar electrophysiology and LUVs is maintained supporting our finding that in the absence of the ^{33}MRDEPI^{38} turn, pores could be efficiently formed, but their activity was not pH dependent. Thus, the short interhelical loop presents a regulatory function and determines the sensibility to pH changes.

Overall, the electrophysiological recordings of peptides inserted in ER-like bilayers are consistent with the formation of a CSFV p7 channel, in which the C-terminal hydrophobic region is a pore lining transmembrane helix and the basic loop regulates the ion permeation process, whereas the N-terminal hydrophobic region functional role remains unknown. In this manner, experiments in planar membranes correlate with previously obtained vesicle leakage results and support the hypothesis

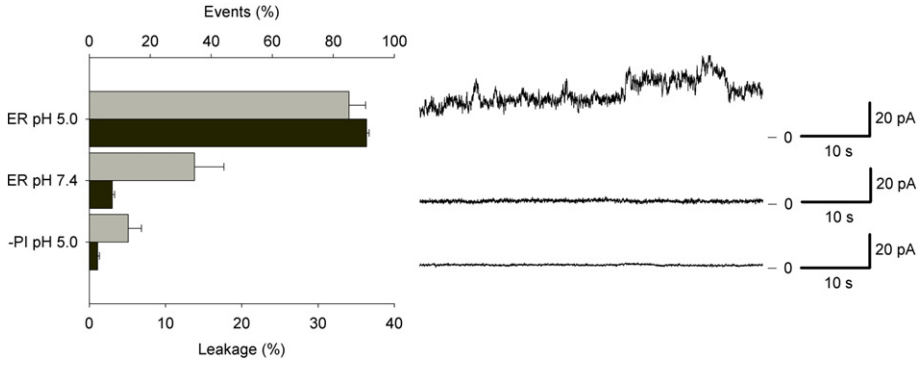

Fig. 3. Comparison between vesicle leakage and channel formation induced by CSFVp7. Left: Percentage of planar bilayers displaying IC activity (light gray) is compared to the leakage percentage induced by CSFV-p7 addition to LUV (protein-to-lipid ratio, 1:250) (dark gray). Right: Representative conductance recordings for the same conditions.

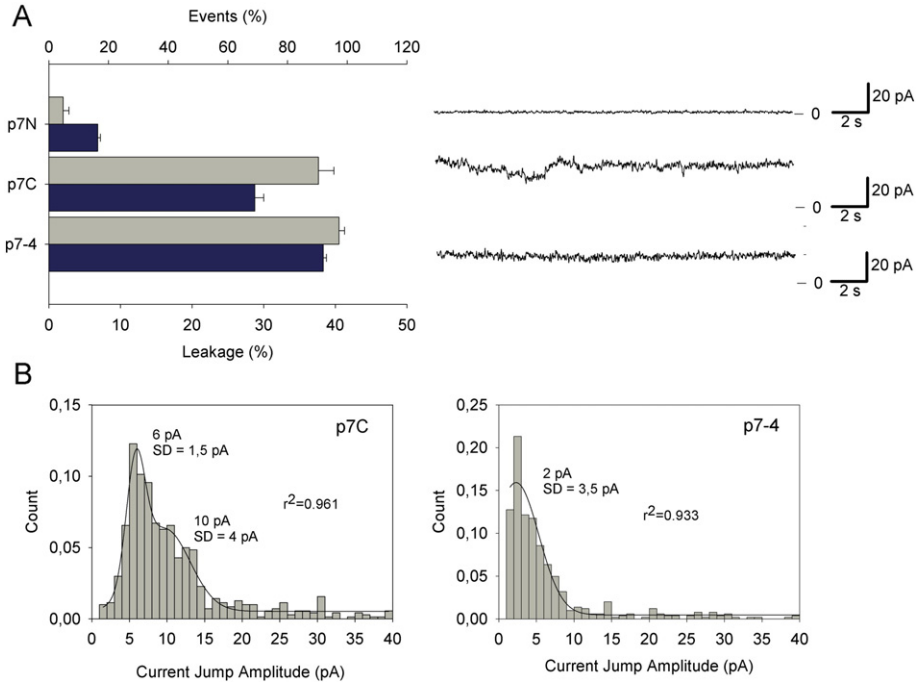

Fig. 4. Pore-forming activity of p7N, p7C and p7-4 peptides in ER-like planar bilayers and vesicles at pH 5.0. A) Left: Comparison of the ability to form channels in planar bilayers (light gray) with leakage induced in LUVs by the addition of p7 peptides to a peptide-to-lipid mole ratio of 1:250 (dark gray). Right: Representative traces of IC activity. B) Histograms of the current jump amplitude measured for the active p7C and p7-4 peptides. The histograms have been fitted to two Gaussian peaks (left panel) and single Gaussian peak (right panel), respectively.

that the same p7 structure could be responsible for both, ion conductance in planar bilayers and ANTS release from vesicles.

3.3. Effects of lipid composition on CSFV-p7 ion channel activity

Results in Figs. 3 and 5 demonstrate that lipid composition has critical effects on the permeabilization induced by CSFV p7 protein and its derived peptides. In the ER-like ternary mixture two conspicuous components, PE and PI, may impart a negative curvature or increase the negative surface charge density of the membrane monolayers, respectively.

Thus, to test intrinsic curvature and surface charge effects on p7full IC activity, we probed a variety of lipid compositions that differed slightly from the canonical ratio 5:3:2 (PC:PE:PI) of ER membranes. Fig. 6 compiles the histograms of current jumps recorded for lipid bilayers made by first keeping constant the amount of charged lipids (PI fixed) and changing the intrinsic curvature (decreasing PC:PE ratio) and then the other way round (i.e., PE fixed and decreasing PC:PI ratio).

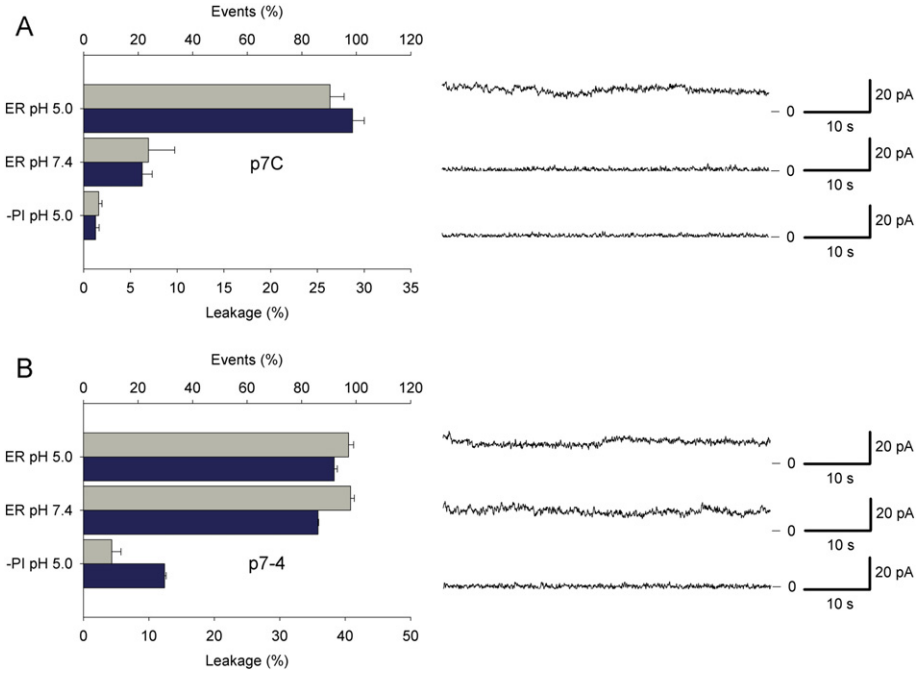

Fig. 5. Comparison between vesicle leakage and channel formation induced by p7C and p7-4 peptides. Effect of pH and lipid composition on IC activity and LUV permeabilization induced by p7C (A) or p7-4 (B). Conditions otherwise as in the previous Fig. 4.

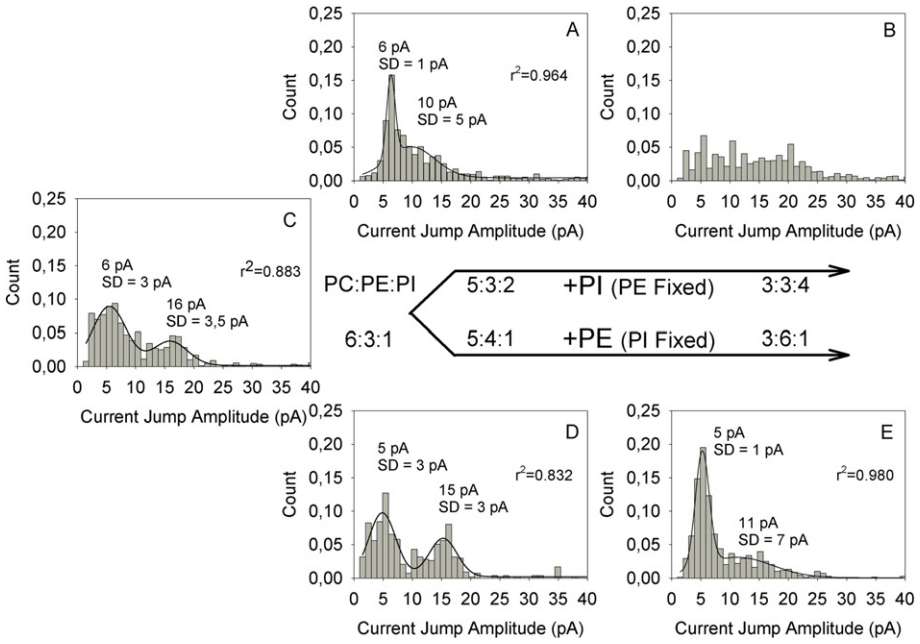

Fig. 6. Histograms of the current jump amplitude measured for the CSFV-p7 protein in different lipid mixtures PC:PE:PI. 5:3:2 (A), 3:3:4 (B), 6:3:1 (C), 5:4:1 (D), 3:6:1 (E). The histograms have been fitted to two Gaussian peaks in all panels but B, where no clear peak is visible.

As previously discussed (Fig. 2B), the main peak at 6 pA and the shoulder at ca. 10 pA observed in the 5:3:2 ER-like composition might denote the prevalence of a single channel, with slight contribution of simultaneous double insertions. As could be expected, [46,47] the effect of the lipid charge in the channel function is remarkable: a decrease in the PI content (6:3:1 and 5:4:1 ratios) enhances a defined second peak in the histogram centered at 15 pA, which comprises current values that triplicate those of the main peak centered at 5 pA. In contrast, the excess of PI (3:3:4) yields a huge dispersion with no clearly defined maximum. On the other hand, altering the intrinsic curvature of the monolayer by including an excess of PE (3:6:1) leads to a single well-defined maximum at 5 pA. This is probably related to the fact that lipids with intrinsic negative curvature, like PE, restrict the formation of protein–lipid combined structures because of the energy penalty involved in the bending of the bilayer leaflet [48]. Notably, the intermediate composition (5:4:1) containing low PI and almost equimolar PC:PE ratio leads to the best definition of the 5 and 15 peaks in the histogram.

The overall understanding of Fig. 6 becomes extremely complex due to the combined action of charge and curvature effects. The only straightforward conclusion that can be drawn is that slight changes in any of these factors yield dramatic changes in the current histograms. In view of that, we see no evident reason to claim that there is a predominant channel structure that depending on the membrane conditions appears only in the form of single channels (5:3:2 or 3:6:1 mixtures) or also in the form of simultaneous multiple insertions (6:3:1 or 5:4:1). Quite the contrary, it seems more likely to suggest that at least two different pore structures can be formed, being the relative abundance and characteristics of each one crucially modulated by the lipid composition in the membrane.

3.4. Identification of two distinct CSFV-p7 ion channel structures

The global analysis of Fig. 6 provides interesting clues but it does not strictly discriminate whether the current jump histograms showing several peaks reveal different pore conformations or alternatively, single and simultaneous multiple insertions of the same pore type. To obtain additional insights on this issue, we analyzed in detail opening and closure events in current traces focusing on the membrane composition of 5:4:1 (PC:PE:PI) that displays the best definition of two different peaks in the corresponding histogram. In Fig. 7 we show representative traces of the two different current states that could be tentatively associated to two distinct oligomerization states or pore structures. In both traces, well-defined “opening” and “closing” current jumps become apparent.

Selectivity experiments carried out in the same lipid mixture 5:4:1 (PC:PE:PI) further supported the existence of two distinct ion-conducting p7 structures (Fig. 8). In the presence of a concentration gradient between both sides of the membrane, there is a net flux of ions through membrane pores and hence an electric current is measured. The applied voltage that is needed to make zero the electric current (the so-called reversal potential, E_{rev}) reveals the preferential passage of either positive or negative ions. In the experimental protocol used here (see the Materials and methods section), a positive applied potential means that the pore is selective to cations and a negative one is associated to an anionic selectivity. We performed reversal potential experiments at pH 5.0 under a concentration ratio of 5 (C_{cis} = 150 mM KCl, C_{trans} = 750 mM KCl) or 10 (C_{cis} = 150 mM KCl, C_{trans} = 1.5 M KCl). Fig. 8 shows the permeability ratio (P_+/P_-) distribution from performed reversal potential experiments. $P_+/P_- > 1$ values are tied to a cationic selectivity whereas lower than 1 values indicate a preference for anions. We see two different groups of values, one connected to a very weak anionic selectivity and other to a cationic one. Note that a cluster of identical small structures displaying a higher

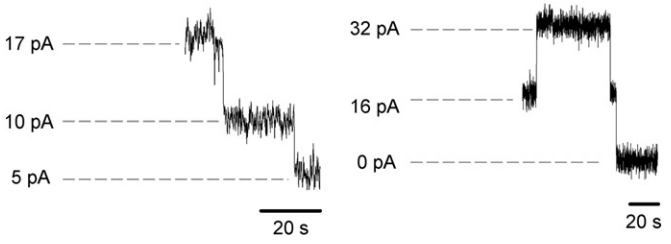

Fig. 7. CSFV-p7 channel current recordings in 150 mM KCl at pH 5 on the membrane composition of 5:4:1 (PC:PE:PI). Traces of two different current state jumps, representatives of two peaks observed in histogram of current jump of 5:4:1 composition shown in previous figure.

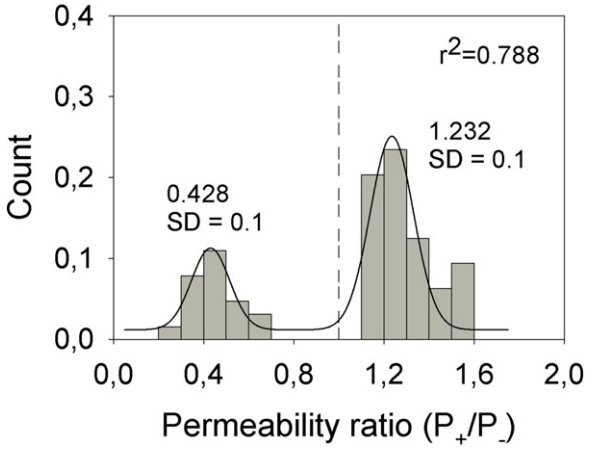

Fig. 8. Histogram of the permeability ratio fitted to two Gaussian peaks. Permeability ratio calculated from reversal potential experiments performed at pH 5.0 under a concentration ratio of 5 (C_{cis} = 150 mM KCl, C_{trans} = 750 mM KCl) or 10 (C_{cis} = 150 mM KCl, C_{trans} = 1.5 M KCl).

conductance would yield the same reversal potential as any of its constituents, not a different value with opposite sign. However, the reason for opposite selectivity in each type of pores remains unclear. This lipid dependence of CSFV p7 protein channel activity resembles that reported for the HCV p7 protein [49] although there are some differences regarding the lipid compositions explored, the sub-conductance states and the cationic selectivity found in that case.

4. Conclusions

Given the great interest in viroporins because of their impact on health of humans and animals, many studies have focused on the ability of viroporins to permeabilize cell membranes by using lipid vesicles as model systems. However, approaches probing their pore-formation mechanisms at the single channel level are still scarce [50]. To this end, we have carried out detailed functional studies contrasting IC activity and leakage experiments using same lipid compositions and subject to the same regulatory factors.

For the particular case of CSFV-p7 viroporin, vesicle assays and electrophysiology in planar bilayers seem different sides of the same coin. Under a variety of conditions we observe a good correspondence between the relative number of channel insertions and the leakage observed in LUVs. In both techniques either the pH or membrane composition are equally critical to regulate the pemeabilization of the membrane system. Remarkably, electrophysiological recordings show reproducible nanometer-sized pores that in accordance with the solved structure for HCV p7 should allow the transport of solvated ions, water and small molecules like ANTS. The pores display mild ion selectivity, compatible with the documented non-specificity of viroporins.

The analysis of CSFV p7 based peptides in planar bilayers is particularly interesting to identify the sequences involved in CSFV-p7 ion channel activity. Thus, the conclusion that the C-terminal hydrophobic region is a pore lining transmembrane helix and the basic loop regulates the pH dependence of the ion permeation process can be firmly established [38]. This is in contrast to what is described for the HCV p7 protein, which contains the pore-forming region at the N-terminus, again emphasizing inter-genus differences among p7 products from the *Flaviviridae* family. In this scheme the functional role of the N-terminal hydrophobic region would remain unknown in the CSFV protein.

Interestingly, lipid modulation of IC activity emerges as a distinctive feature of some viroporins. In the case of CSFV p7, minimal changes in either the lipid charge or the intrinsic lipid curvature originates dramatic changes in the current histograms. The lack of structural information about CSFV-p7 viroporin makes difficult even a qualitative explanation of the lipid regulation the IC activity. The combined analysis of current traces and selectivity experiments indicates that different current states would probably correspond to, at least, two different independent pore structures.

Author declaration

We wish to confirm that there are no known conflicts of interest associated with this publication and there has been no significant financial support for this work that could have influenced its outcome.

Acknowledgments

The authors acknowledge financial support by the Spanish Ministry of Economy and Competitiveness (MINECO Project FIS2013-40473-P), Fundació Caixa Castelló-Bancaixa (Project no. P1-1B2012-03), the Agricultural Research Service of the US (ARS-USDA Project 8064-32000-056-18S to EL and JLN) and the Basque Government (Project IT838-13 to JLN). We thank Dr. Manuel Borca (Plum Island Animal Disease Center, ARS, USDA) for the provision of p7 protein and derived peptides used in this study.

References

[1] L. Carrasco, L. Pérez, A. Irurzun, J. Lama, F. Martínez-Abarca, P. Rodríguez, R. Guinea, J. Castrillo, M. Angel, M. José, Modification of Membrane Permeability by Animal Viruses, in: L. Carrasco, N. Sonenberg, E. Wimmer (Eds.), Regulation of Gene Expression in Animal Viruses, 240, Springer US 1993, pp. 283–303.
[2] J.L. Nieva, V. Madan, L. Carrasco, Viroporins: structure and biological functions, Nat. Rev. Microbiol. 10 (2012) 563–574.
[3] C. Sze, Y.J. Tan, Viral membrane channels: role and function in the virus life cycle, Viruses 7 (2015) 3261–3284.
[4] S. Grambas, M.S. Bennett, A.J. Hay, Influence of amantadine resistance mutations on the pH regulatory function of the M2 protein of influenza A viruses, Virology 191 (1992) 541–549.
[5] L.H. Pinto, G.R. Dieckmann, C.S. Gandhi, C.G. Papworth, J. Braman, M.A. Shaughnessy, J.D. Lear, R.A. Lamb, W.F. DeGrado, A functionally defined model for the M2 proton channel of influenza A virus suggests a mechanism for its ion selectivity, Proc. Natl. Acad. Sci. U. S. A. 94 (1997) 11301–11306.
[6] E.K. Park, M.R. Castrucci, A. Portner, Y. Kawaoka, The M2 ectodomain is important for its incorporation into influenza A virions, J. Virol. 72 (1998) 2449–2455.
[7] J.S. Rossman, X. Jing, G.P. Leser, V. Balannik, L.H. Pinto, R.A. Lamb, Influenza virus M2 ion channel protein is necessary for filamentous virion formation, J. Virol. 84 (2010) 5078–5088.
[8] A.M. Atoom, D.M. Jones, R.S. Russell, Evidence suggesting that HCV p7 protects E2 glycoprotein from premature degradation during virus production, Virus Res. 176 (2013) 199–210.
[9] C. Brohm, E. Steinmann, M. Friesland, I.C. Lorenz, A. Patel, F. Penin, R. Bartenschlager, T. Pietschmann, Characterization of determinants important for hepatitis C virus p7 function in morphogenesis by using trans-complementation, J. Virol. 83 (2009) 11682–11693.
[10] A. Sakai, M.S. Claire, K. Faulk, S. Govindarajan, S.U. Emerson, R.H. Purcell, J. Bukh, The p7 polypeptide of hepatitis C virus is critical for infectivity and contains functionally important genotype-specific sequences, Proc. Natl. Acad. Sci. U. S. A. 100 (2003) 11646–11651.
[11] C.T. Jones, C.L. Murray, D.K. Eastman, J. Tassello, C.M. Rice, Hepatitis C virus p7 and NS2 proteins are essential for production of infectious virus, J. Virol. 81 (2007) 8374–8383.
[12] E. Steinmann, F. Penin, S. Kallis, A.H. Patel, R. Bartenschlager, T. Pietschmann, Hepatitis C virus p7 protein is crucial for assembly and release of infectious virions, PLoS Pathog. 3 (2007), e103.
[13] R.L. Willey, F. Maldarelli, M.A. Martin, K. Strebel, Human immunodeficiency virus type 1 Vpu protein induces rapid degradation of CD4, J. Virol. 66 (1992) 7193–7200.
[14] N. Van Damme, D. Goff, C. Katsura, R.L. Jorgenson, R. Mitchell, M.C. Johnson, E.B. Stephens, J. Guatelli, The interferon-induced protein BST-2 restricts HIV-1 release and is downregulated from the cell surface by the viral Vpu protein, Cell Host Microbe 3 (2008) 245–252.
[15] M. Moll, S.K. Andersson, A. Smed-Sorensen, J.K. Sandberg, Inhibition of lipid antigen presentation in dendritic cells by HIV-1 Vpu interference with CD1d recycling from endosomal compartments, Blood 116 (2010) 1876–1884.
[16] A.H. Shah, B. Sowrirajan, Z.B. Davis, J.P. Ward, E.M. Campbell, V. Planelles, E. Barker, Degranulation of natural killer cells following interaction with HIV-1-infected cells is hindered by downmodulation of NTB-A by Vpu, Cell Host Microbe 8 (2010) 397–409.
[17] S.J. Neil, T. Zang, P.D. Bieniasz, Tetherin inhibits retrovirus release and is antagonized by HIV-1 Vpu, Nature 451 (2008) 425–430.
[18] V. Madan, S. Sanchez-Martinez, N. Vedovato, G. Rispoli, L. Carrasco, J.L. Nieva, Plasma membrane-porating domain in poliovirus 2B protein. A short peptide mimics viroporin activity, J. Mol. Biol. 374 (2007) 951–964.

[19] J.L. Nieva, A. Agirre, S. Nir, L. Carrasco, Mechanisms of membrane permeabilization by picornavirus 2B viroporin, FEBS Lett. 552 (2003) 68–73.
[20] R. Aldabe, A. Irurzun, L. Carrasco, Poliovirus protein 2BC increases cytosolic free calcium concentrations, J. Virol. 71 (1997) 6214–6217.
[21] A.S. de Jong, H.J. Visch, F. de Mattia, M.M. van Dommelen, H.G. Swarts, T. Luyten, G. Callewaert, W.J. Melchers, P.H. Willems, F.J. van Kuppeveld, The coxsackievirus 2B protein increases efflux of ions from the endoplasmic reticulum and Golgi, thereby inhibiting protein trafficking through the Golgi, J. Biol. Chem. 281 (2006) 14144–14150.
[22] L. Martinez-Gil, I. Mingarro, Viroporins, examples of the two-stage membrane protein folding model, Viruses 7 (2015) 3462–3482.
[23] M. Campanella, A.S. de Jong, K.W. Lanke, W.J. Melchers, P.H. Willems, P. Pinton, R. Rizzuto, F.J. van Kuppeveld, The coxsackievirus 2B protein suppresses apoptotic host cell responses by manipulating intracellular Ca^{2+} homeostasis, J. Biol. Chem. 279 (2004) 18440–18450.
[24] A.L. Wozniak, S. Griffin, D. Rowlands, M. Harris, M. Yi, S.M. Lemon, S.A. Weinman, Intracellular proton conductance of the hepatitis C virus p7 protein and its contribution to infectious virus production, PLoS Pathog. 6 (2010), e1001087.
[25] E. Alvarado-Facundo, Y. Gao, R.M. Ribas-Aparicio, A. Jimenez-Alberto, C.D. Weiss, W. Wang, Influenza virus M2 protein ion channel activity helps to maintain pandemic 2009 H1N1 virus hemagglutinin fusion competence during transport to the cell surface, J. Virol. 89 (2015) 1975–1985.
[26] T. Sakaguchi, G.P. Leser, R.A. Lamb, The ion channel activity of the influenza virus M2 protein affects transport through the Golgi apparatus, J. Cell Biol. 133 (1996) 733–747.
[27] K. Takeuchi, R.A. Lamb, Influenza virus M2 protein ion channel activity stabilizes the native form of fowl plague virus hemagglutinin during intracellular transport, J. Virol. 68 (1994) 911–919.
[28] L.H. Pinto, L.J. Holsinger, R.A. Lamb, Influenza virus M2 protein has ion channel activity, Cell 69 (1992) 517–528.
[29] D. Pavlovic, D.C. Neville, O. Argaud, B. Blumberg, R.A. Dwek, W.B. Fischer, N. Zitzmann, The hepatitis C virus p7 protein forms an ion channel that is inhibited by long-alkyl-chain iminosugar derivatives, Proc. Natl. Acad. Sci. U. S. A. 100 (2003) 6104–6108.
[30] S.D. Griffin, L.P. Beales, D.S. Clarke, O. Worsfold, S.D. Evans, J. Jaeger, M.P. Harris, D.J. Rowlands, The p7 protein of hepatitis C virus forms an ion channel that is blocked by the antiviral drug, amantadine, FEBS Letters 535 (2003) 34–38.
[31] S.D. Griffin, R. Harvey, D.S. Clarke, W.S. Barclay, M. Harris, D.J. Rowlands, A conserved basic loop in hepatitis C virus p7 protein is required for amantadine-sensitive ion channel activity in mammalian cells but is dispensable for localization to mitochondria, J. Gen. Virol. 85 (2004) 451–461.
[32] C. Verdia-Baguena, J.L. Nieto-Torres, A. Alcaraz, M.L. Dediego, L. Enjuanes, V.M. Aguilella, Analysis of SARS-CoV E protein ion channel activity by tuning the protein and lipid charge, Biochim. Biophys. Acta 1828 (2013) 2026–2031.
[33] R. Montserret, N. Saint, C. Vanbelle, A.G. Salvay, J.P. Simorre, C. Ebel, N. Sapay, J.G. Renisio, A. Bockmann, E. Steinmann, T. Pietschmann, J. Dubuisson, C. Chipot, F. Penin, NMR structure and ion channel activity of the p7 protein from hepatitis C virus, J. Biol. Chem. 285 (2010) 31446–31461.
[34] A. Premkumar, L. Wilson, G.D. Ewart, P.W. Gage, Cation-selective ion channels formed by p7 of hepatitis C virus are blocked by hexamethylene amiloride, FEBS Lett. 557 (2004) 99–103.
[35] T. Mehnert, A. Routh, P.J. Judge, Y.H. Lam, D. Fischer, A. Watts, W.B. Fischer, Biophysical characterization of Vpu from HIV-1 suggests a channel-pore dualism, Proteins 70 (2008) 1488–1497.
[36] S.W. Gan, W. Surya, A. Vararattanavech, J. Torres, Two different conformations in hepatitis C virus p7 protein account for proton transport and dye release, PLoS One 9 (2014), e78494.
[37] A. Agirre, M. Lorizate, S. Nir, J.L. Nieva, Poliovirus 2b insertion into lipid monolayers and pore formation in vesicles modulated by anionic phospholipids, Biochim. Biophys. Acta 1778 (2008) 2621–2626.
[38] D.P. Gladue, L.G. Holinka, E. Largo, I. Fernandez Sainz, C. Carrillo, V. O'Donnell, R. Baker-Branstetter, Z. Lu, X. Ambroggio, G.R. Risatti, J.L. Nieva, M.V. Borca, Classical swine fever virus p7 protein is a viroporin involved in virulence in swine, J. Virol. 86 (2012) 6778–6791.
[39] A. Alcaraz, E.M. Nestorovich, M.L. Lopez, E. Garcia-Gimenez, S.M. Bezrukov, V.M. Aguilella, Diffusion, exclusion, and specific binding in a large channel: a study of OmpF selectivity inversion, Biophys. J. 96 (2009) 56–66.
[40] M.J. Hope, M.B. Bally, G. Webb, P.R. Cullis, Production of large unilamellar vesicles by a rapid extrusion procedure: characterization of size distribution, trapped volume and ability to maintain a membrane potential, Biochim. Biophys. Acta 812 (1985) 55–65.
[41] H. Ellens, J. Bentz, F.C. Szoka, H^+- and Ca^{2+}-induced fusion and destabilization of liposomes, Biochemistry 24 (1985) 3099–3106.
[42] E. Largo, D.P. Gladue, N. Huarte, M.V. Borca, J.L. Nieva, Pore-forming activity of pestivirus p7 in a minimal model system supports genus-specific viroporin function, Antivir. Res. 101 (2014) 30–36.
[43] G. van Meer, D.R. Voelker, G.W. Feigenson, Membrane lipids: where they are and how they behave, Nat. Rev. Mol. Cell Biol. 9 (2008) 112–124.
[44] H. Nikaido, Molecular basis of bacterial outer membrane permeability revisited, Microbiol. Mol. Biol. Rev. 67 (2003) 593–656.
[45] B. Hille, Ion Channels of Excitable Membranes, 3rd ed. Sinauer Associates, Sunderland, Mass., 2001
[46] T.K. Rostovtseva, V.M. Aguilella, I. Vodyanoy, S.M. Bezrukov, V.A. Parsegian, Membrane surface-charge titration probed by gramicidin A channel conductance, Biophys. J. 75 (1998) 1783–1792.
[47] V.M. Aguilella, C. Verdia-Baguena, A. Alcaraz, Lipid charge regulation of non-specific biological ion channels, Phys. Chem. Chem. Phys. 16 (2014) 3881–3893.
[48] A.A. Sobko, E.A. Kotova, Y.N. Antonenko, S.D. Zakharov, W.A. Cramer, Lipid dependence of the channel properties of a colicin E1-lipid toroidal pore, J. Biol. Chem. 281 (2006) 14408–14416.
[49] T. Whitfield, A.J. Miles, J.C. Scheinost, J. Offer, P. Wentworth Jr., R.A. Dwek, B.A. Wallace, P.C. Biggin, N. Zitzmann, The influence of different lipid environments on the structure and function of the hepatitis C virus p7 ion channel protein, Mol. Membr. Biol. 28 (2011) 254–264.
[50] J. Nieto-Torres, C. Verdiá-Báguena, C. Castaño-Rodriguez, V. Aguilella, L. Enjuanes, Relevance of viroporin ion channel activity on viral replication and pathogenesis, Viruses 7 (2015) 2786.